Doppler backscattering for spherical tokamaks, the collisionality dependence of intrinsic rotation, & a novel cross-polarization scattering technique

Presented at
NSTX-U Physics Meeting
Princeton, NJ, USA
July 28, 2014

Presented by
J.C. Hillesheim[1]

in collaboration with
M. Barnes[2,1], M. Carr[1], N.A. Crocker[3],
D. Dunai[4], A.R. Field[1], A. Kirk[1], N. Hawkes[1],
H. Meyer[1], A. Meakins[1], F.I. Parra[2,1], W.A. Peebles[3],
R. Scannell[1], A. Thornton[1], and the MAST Team[1]

[1] Culham Centre for Fusion Energy, UK
[2] University of Oxford, UK
[3] University of California, Los Angeles, USA
[4] Wigner Research Centre for Physics, Hungary

Research Councils UK Energy For a Low Carbon Future

CCFE is the fusion research arm of the **United Kingdom Atomic Energy Authority**

CCFE CULHAM CENTRE FOR FUSION ENERGY

Summary

- Doppler backscattering (DBS) for spherical tokamaks
  - DBS implemented for MAST
- Dependence of intrinsic rotation on collisionality in MAST
- Cross-polarization DBS and microtearing modes (MTM) at the top of the MAST H-mode pedestal

Mega Amp Spherical Tokamak

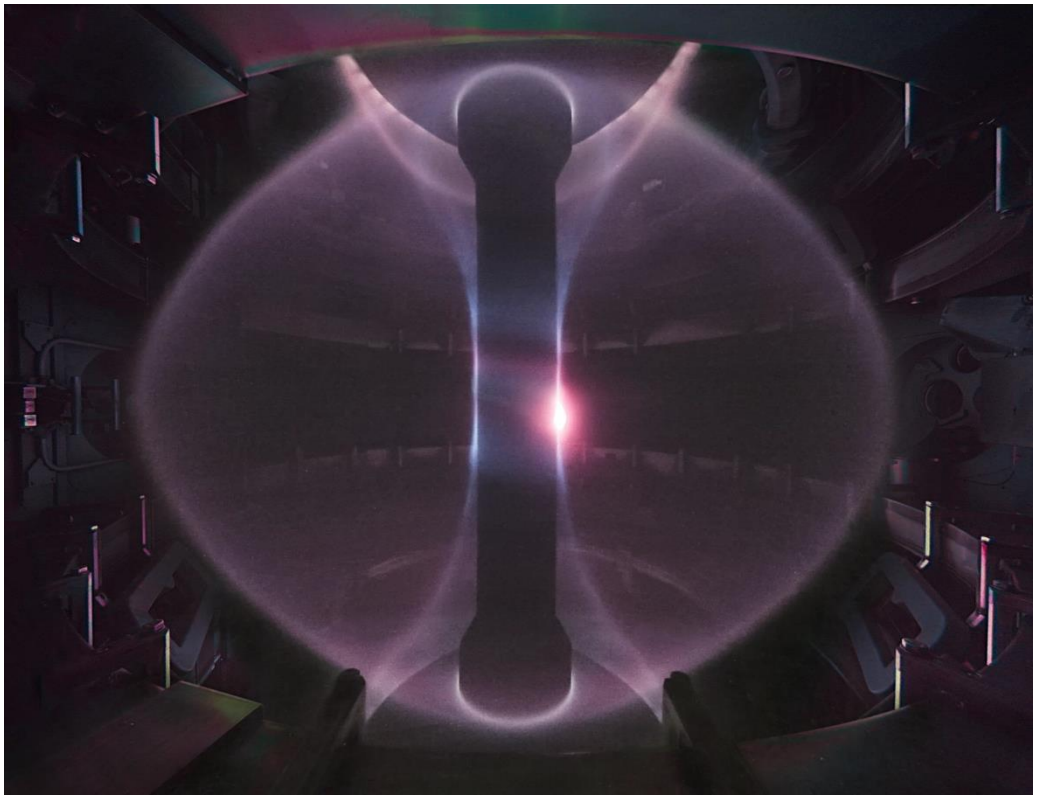

- MAST is an experiment at CCFE
- R≈0.9 m, a ≈ 0.4 m
- Toroidal field 0.5 T
- Up to 1 MA plasma current and ~4 MW NBI

International Collaboration between CCFE and UCLA to implement DBS for MAST

- Two 8-channel systems installed at NSTX and used for reflectometry (Crocker PPCF 2011)
  - Q-band 30-50 GHz
  - V-band 55-75 GHz
- NSTX under construction for upgrade in 2013
- Hardware moved to Culham for temporary installation on MAST

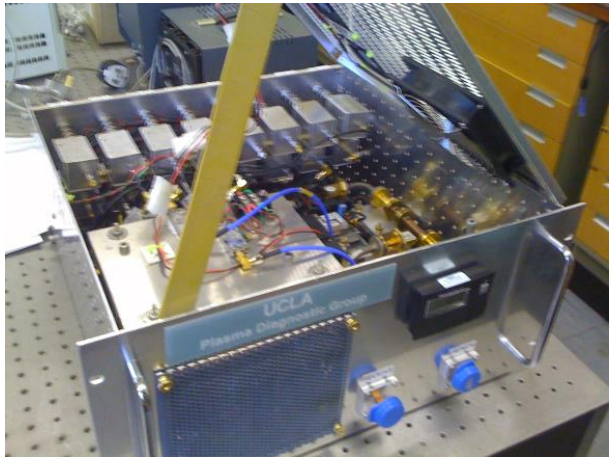

DBS at MAST installed through collaboration with UCLA and supported by the US DOE

Doppler backscattering measures the *radially localized* lab frame velocity and density fluctuation level

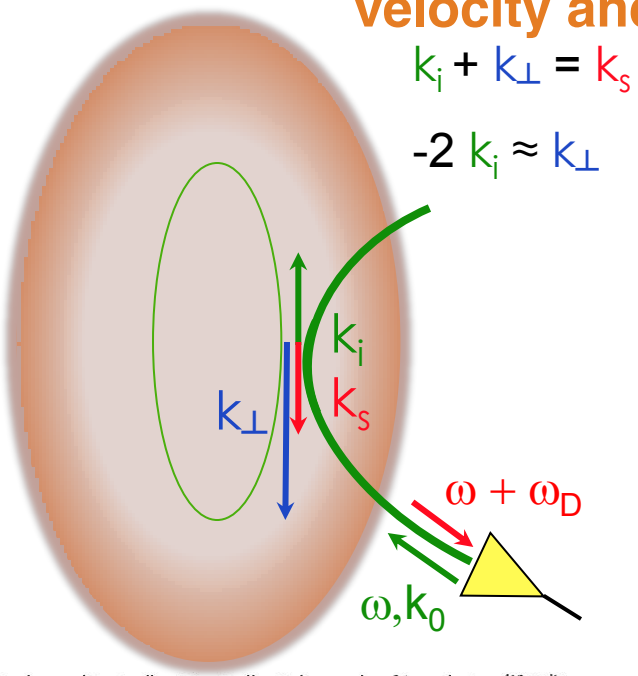

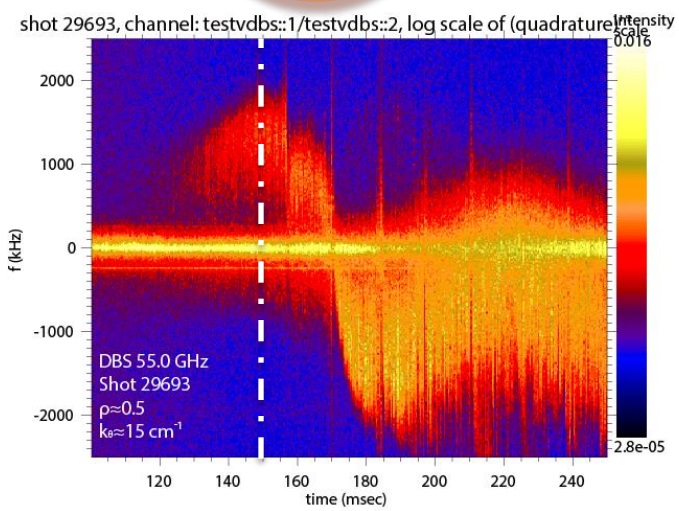

NBI from 150 ms

- A localized scattering region is created near the cutoff
- Amplitude of backscattered signal related to fluctuation level of intermediate-k density fluctuations ($k_\perp \rho_i \sim$ 2-15, $k_\perp \sim$ 4-24 cm^{-1})
  - Wavenumber can be selected by changing launch angle
- Doppler shift in backscattered signal induced by lab frame velocity of the turbulence

$$\omega_D \approx k_\perp v_{Lab}$$

$$v_{Lab} = v_{E\times B} + \tilde{v}$$

PART I:

DBS for Spherical Tokamaks

Sub ion-scale turbulence often important in tokamaks

- In MAST H-mode plasmas, ion-scale turbulence measurements typically very small
  - Ion heat transport often near neoclassical in spherical tokamak H-modes
- Strong beam heating in standard tokamaks often drives large ExB shear, suppressing ion scales
  - e.g. Schmitz NF 2012 at right

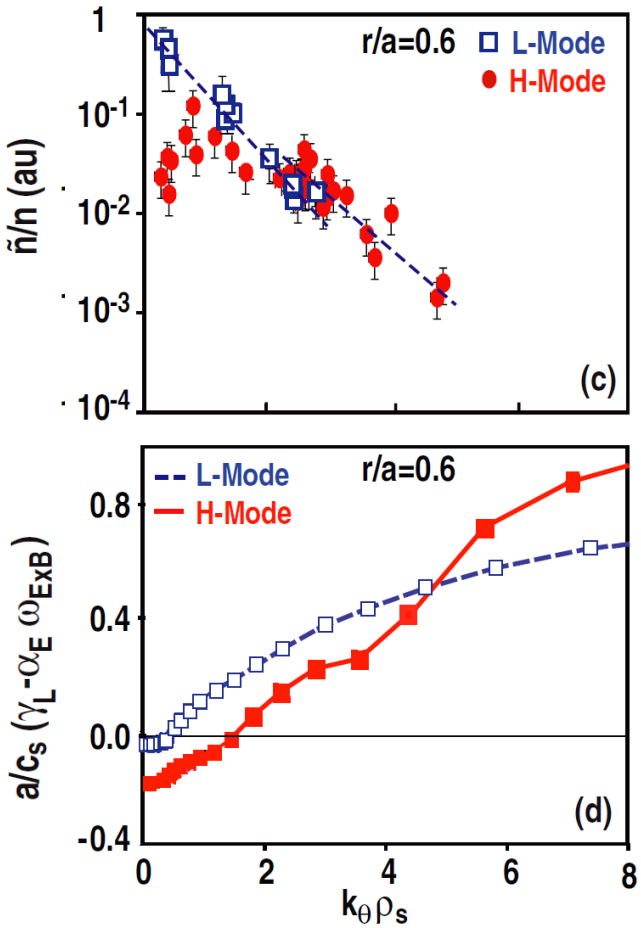

Scattering formalism yields constraint on alignment between incident wave and density fluctuations for 180° backscattering

- Following from, e.g. Bekefi, *Radiation Processes in Plasmas,* 1966, Slusher and Surko Phys. Fluids 1980:

$$\mathbf{E_s}(\omega_s) = \left[\hat{\mathbf{k}}_s \times \left(\hat{\mathbf{k}}_s \times \mathbf{E_0}\right)\right] \frac{r_0}{16\pi^4\sqrt{a_x a_y}} \int d\omega_n dt d\mathbf{k}_n d\mathbf{x}$$

$$\widetilde{n}(\mathbf{k_n}, \omega_n) e^{-x^2/a_x^2} e^{-y^2/a_y^2} e^{-i(\omega_i+\omega_n-\omega_s)t} e^{i(\mathbf{k}_i+\mathbf{k}_n-\mathbf{k}_s)\mathbf{x}} e^{-i\omega_s R/c} + \text{c.c.}$$

$$dI \propto dz\, \widetilde{n}^2(\mathbf{k_n}, z) \exp\left(-\frac{(k_{n,x}-k_{s,x})^2 a_x^2}{2}\right) \exp\left(-\frac{(k_{n,y}-k_{s,y})^2 a_y^2}{2}\right)$$

$$k_{||} << k_\perp \qquad \hat{\mathbf{k}}_s \cdot \hat{\mathbf{B}} = \cos(\pi/2 - \theta_{mis})$$

$$dI \propto dz\, \widetilde{n}^2(\mathbf{k_n}, z) \exp\left(-\frac{|\mathbf{k}_s|^2 a_0^2 \sin^2\theta_{mis}}{2}\right)$$

$$|\theta_{mis}| \lesssim \frac{2\sqrt{2}}{k_n a_0}$$

Broad profile access possible

- The two 8-channel systems, originally designed for NSTX, provided broad profile access in MAST
- L-mode: most of minor radius usually covered
- Sometimes limited core access in H-mode due to flat density profiles, bat-eared profiles

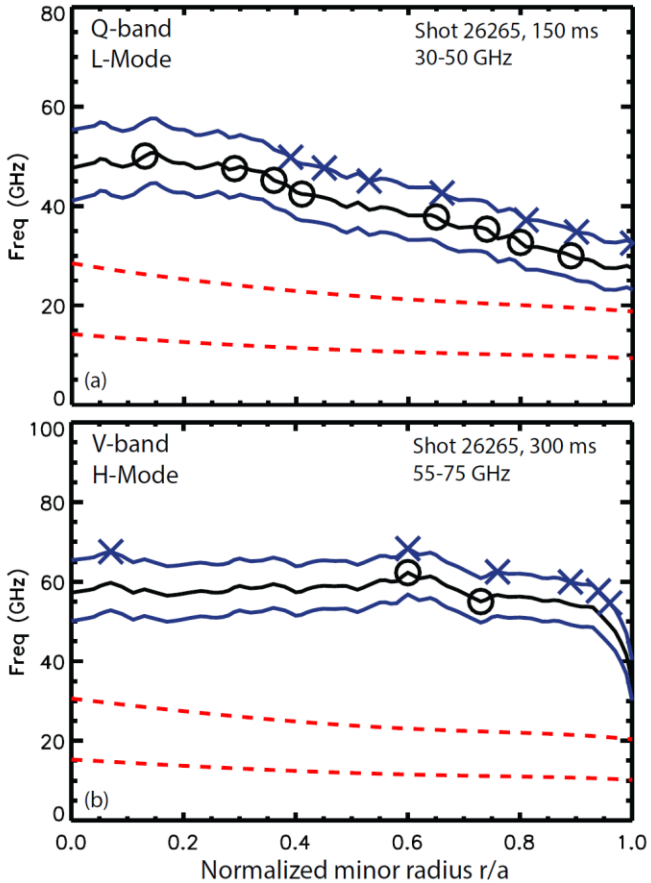

Ray tracing used to assess design and for data analysis

- EFIT and density profile from Thomson scattering used as inputs for Genray
- Mismatch angle, scattering wavenumber, and scattering location determined from ray tracing output

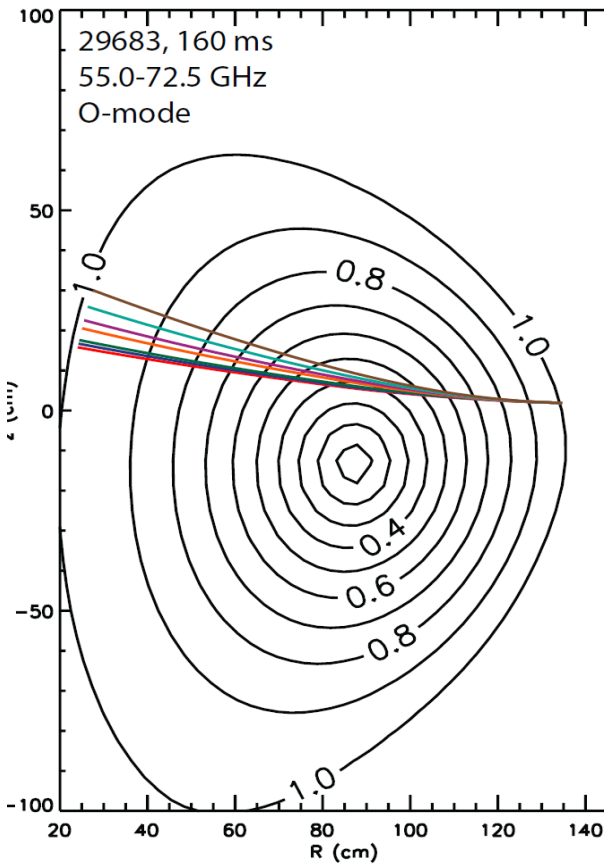

Raying tracing for design showed 2D steering was necessary

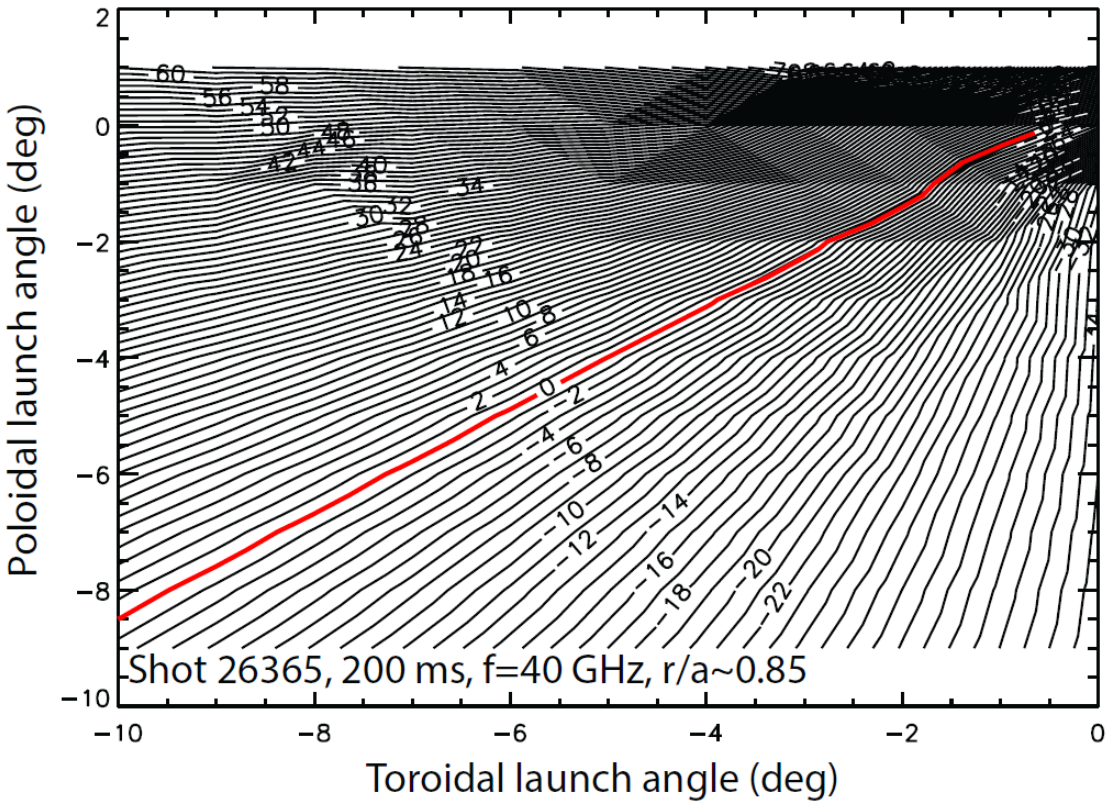

$$|\theta_{mis}| \lesssim \frac{2\sqrt{2}}{k_n a_0}$$

Toroidal launch angle dependence strongly impacts mismatch angle

- Scattering condition highly sensitive to toroidal launch angle
- Scattering wavenumber dominantly determined by poloidal launch angle

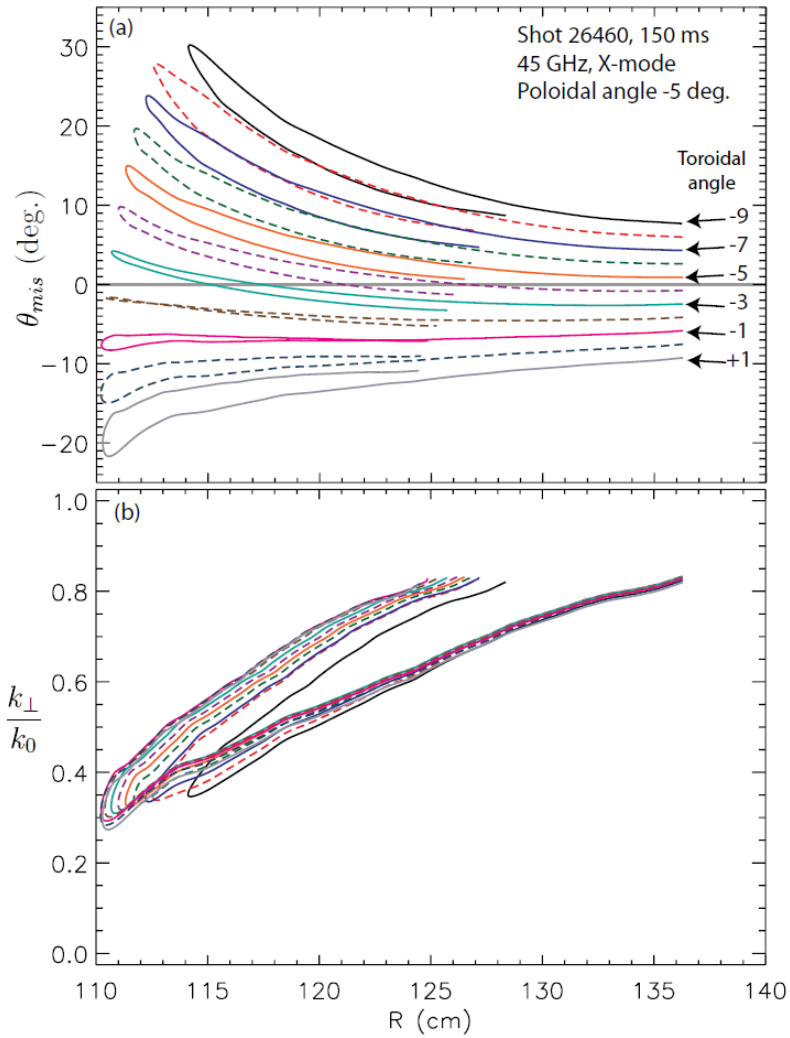

Scattering alignment changes with radius

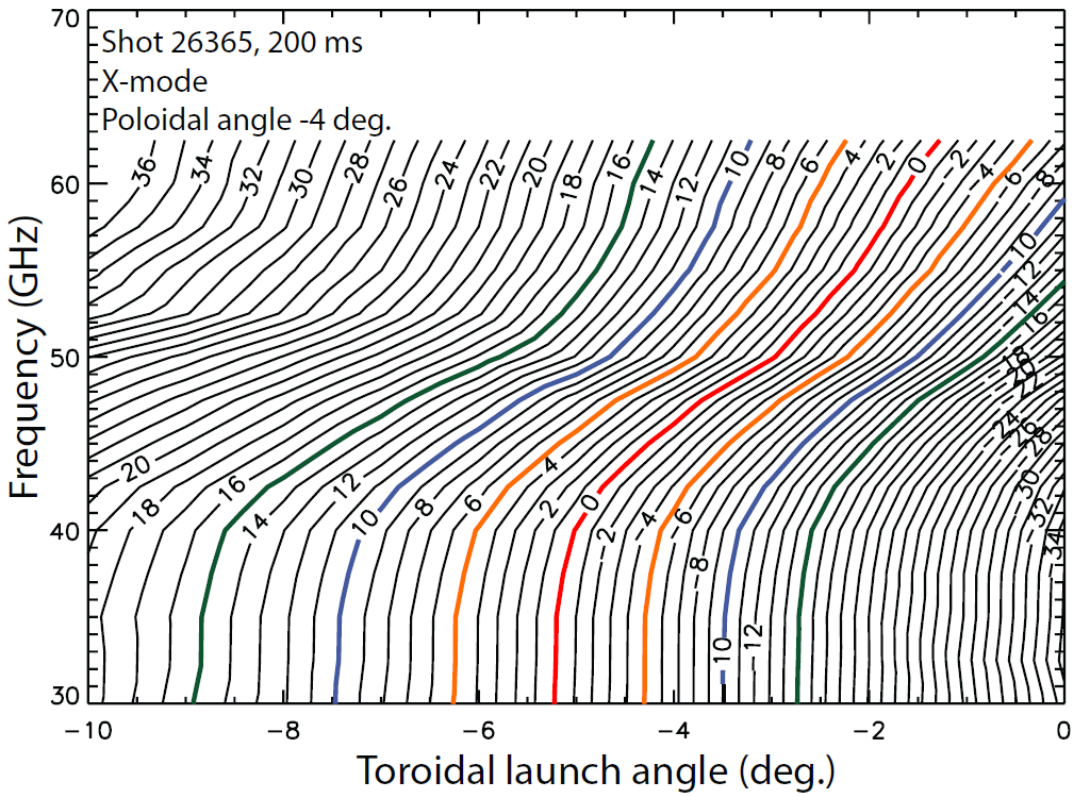

$$|\theta_{mis}| \lesssim \frac{2\sqrt{2}}{k_n a_0}$$

- Not possible to pick one angle that works for all radial positions
- Depends on local magnetic pitch angle

Scattering alignment changes with time

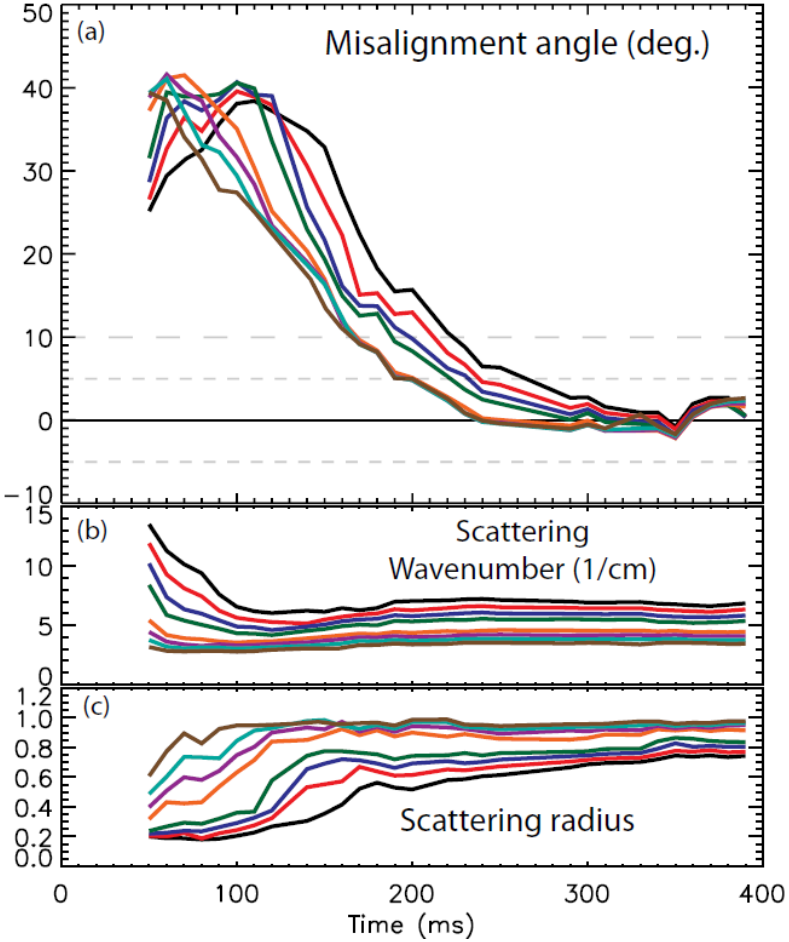

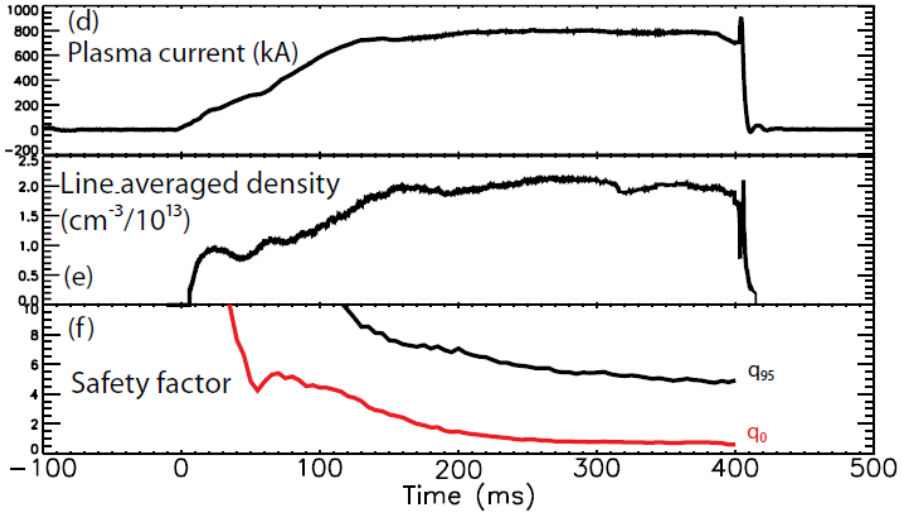

- **Expect no signal early in shot,** followed by scattering coming into alignment later

Quasi-optical Gaussian beam system to combine DBS systems and for 2D steering

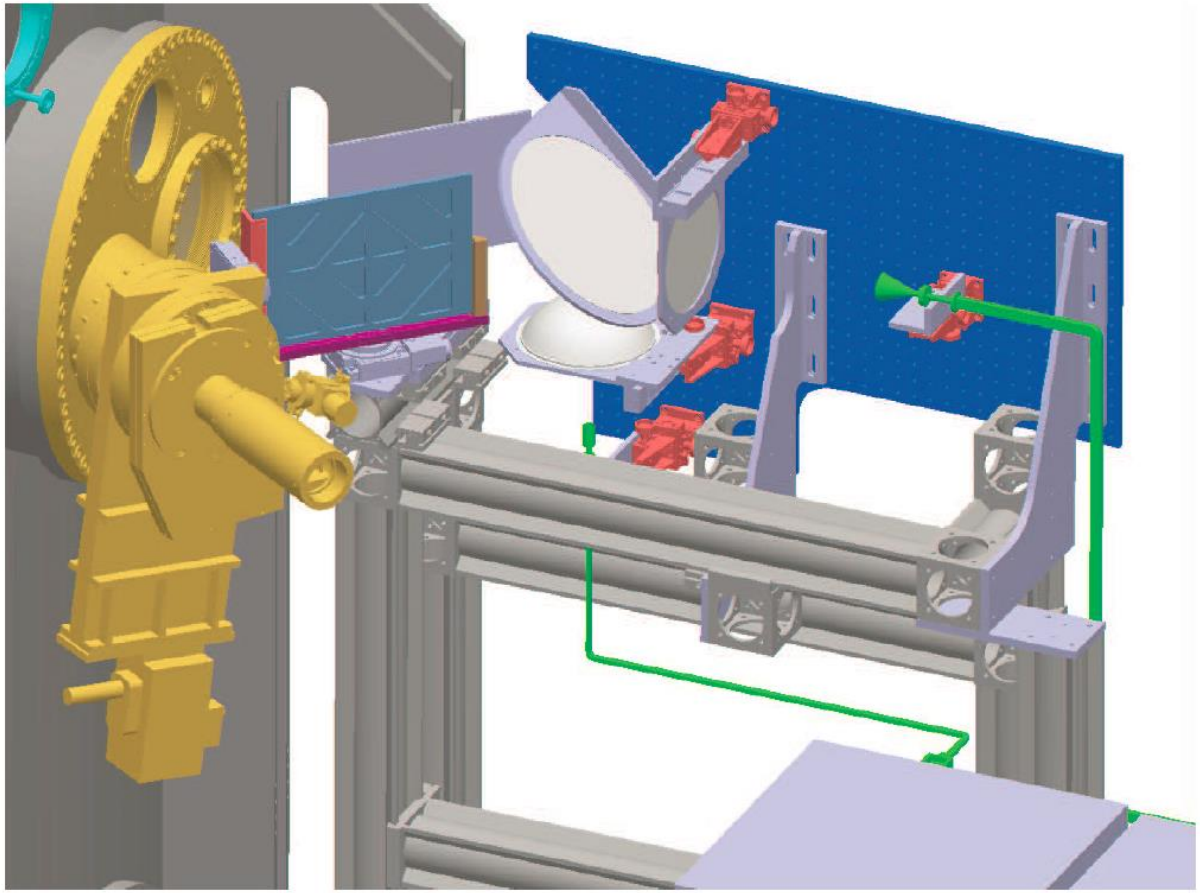

Toroidal angle scan in repeated plasma conditions test design expectations

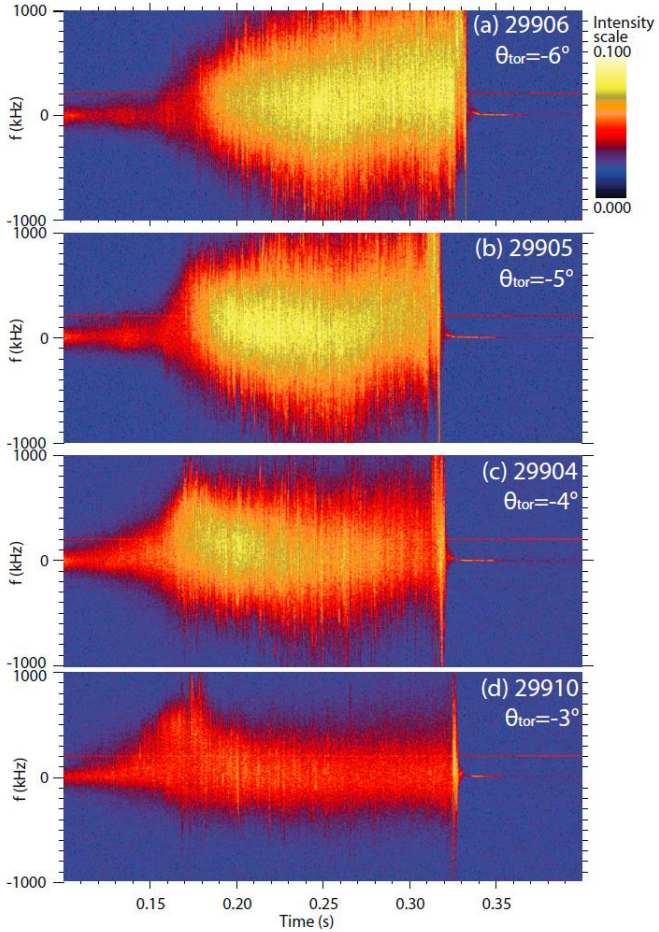

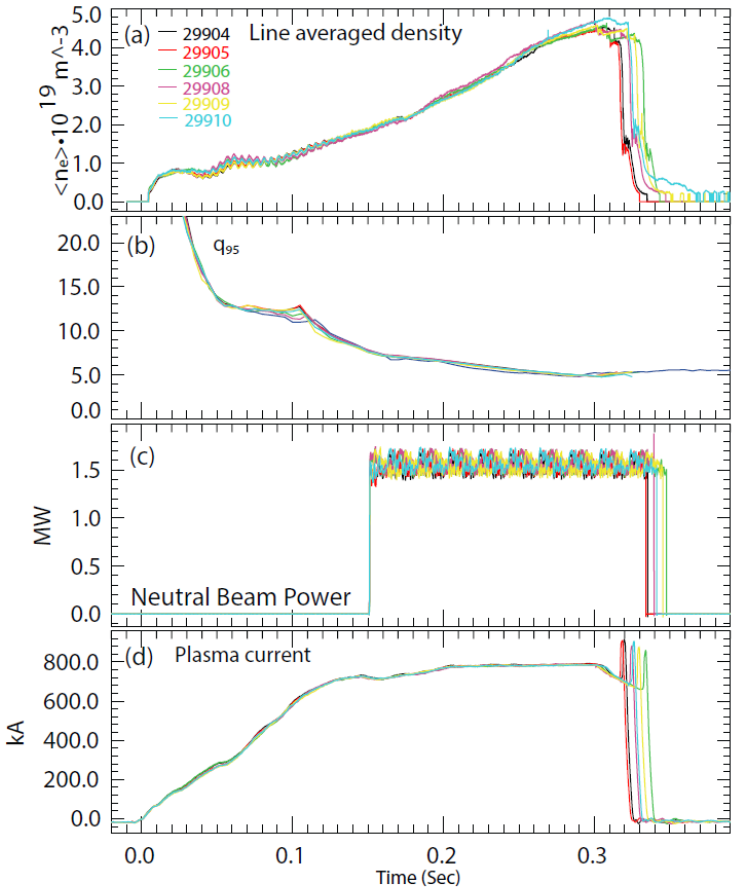

Scattered power depends on toroidal launch angle

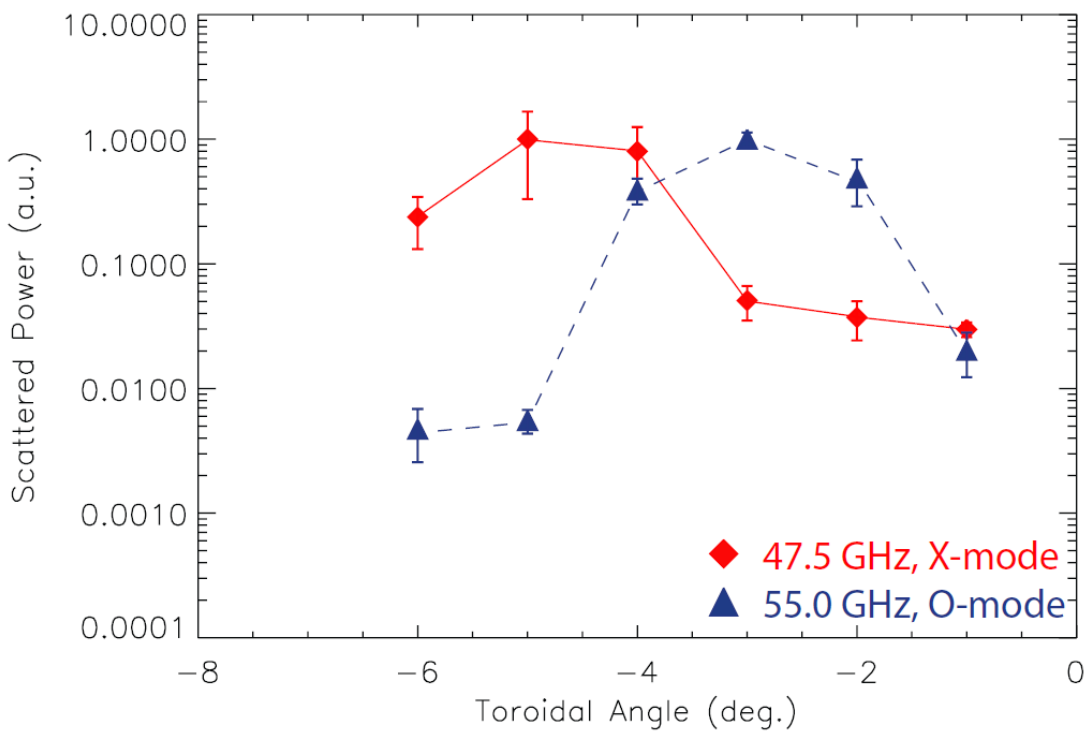

- Demonstrates sensitivity to local pitch angle
- t=190 ms
- 47.5 GHz
  - r/a ≈ 0.90
  - k ≈ 7 cm^{-1}
- 55.0 GHz
  - r/a ≈ 0.70
  - k ≈ 9 cm^{-1}
- Further work needed for k-spectra

Comparison of scattered power to scattering mismatch angle

- A toroidal offset was apparent in experimental data
- By comparison to calculations, offset determined to be 2° ± 1°
- Further analysis of this data set necessary for comparisons of fluctuation amplitudes
  - Wavenumber insensitive to offset

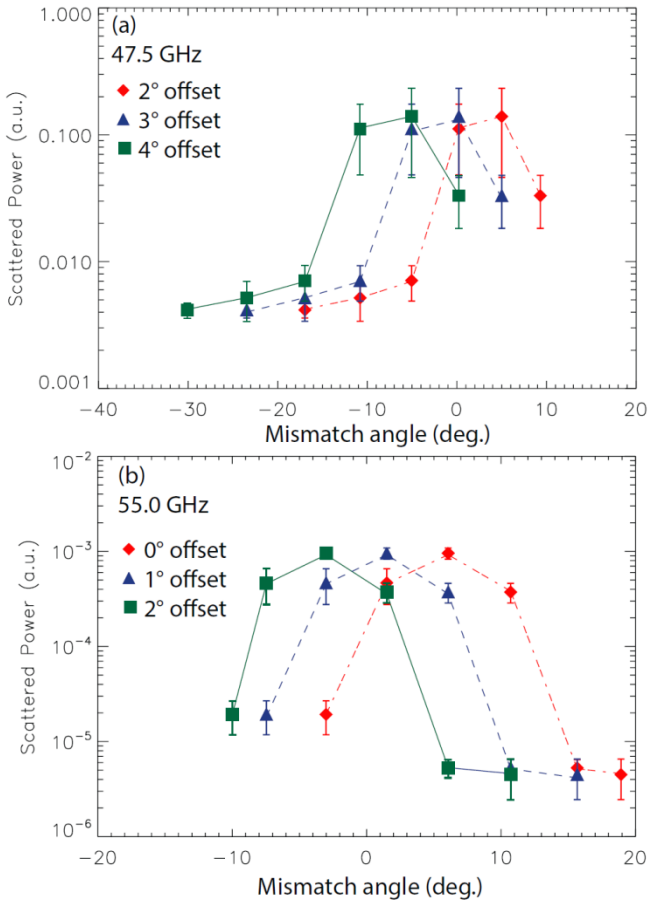

2D steering enables High-k DBS

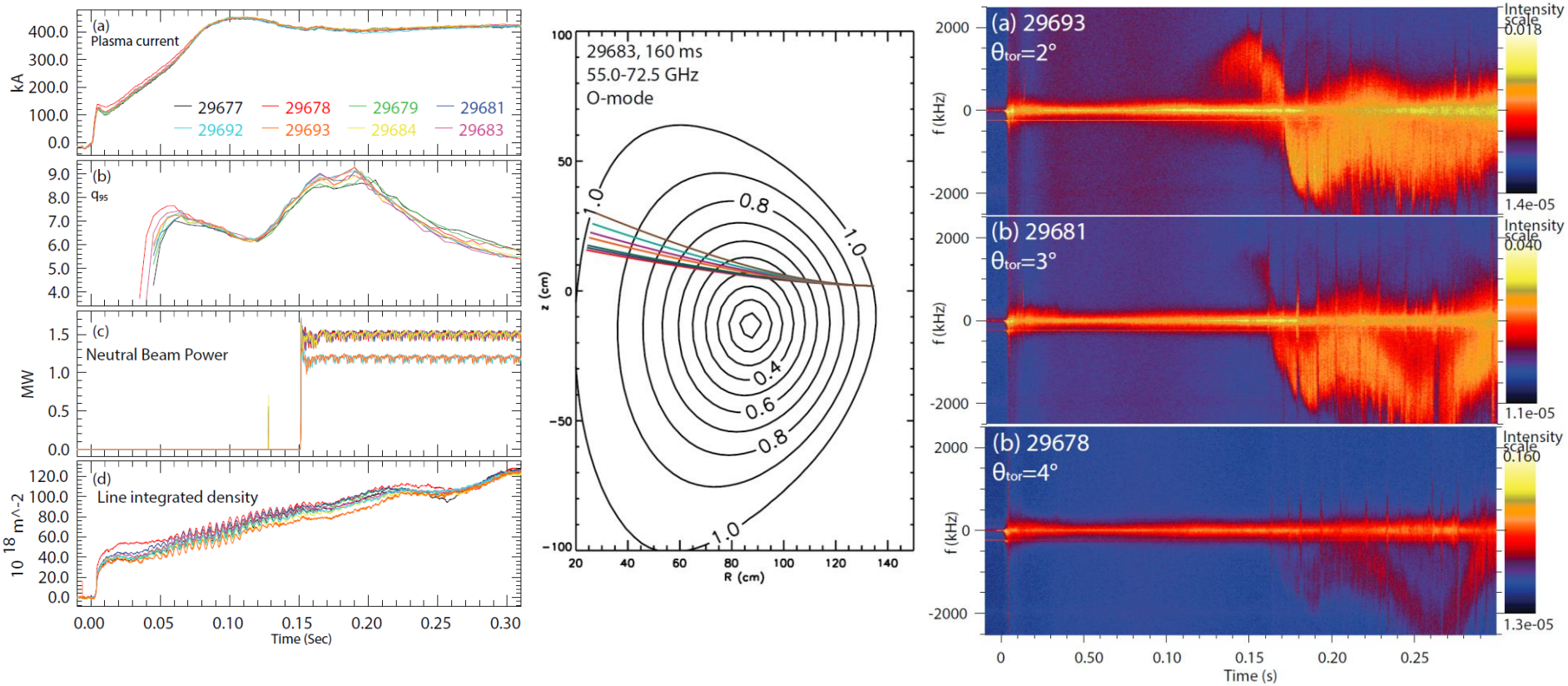

- Core measurements **up to 24 cm^{-1}** ($k_\perp \rho_i$ ~15) at 72.5 GHz

Cross-diagnostic comparisons verify design and analysis

- Shot with an ITB chosen for cross-diagnostic comparisons
- L-mode with good profile access for DBS
- Strong ion pressure gradient contributes to radial electric field

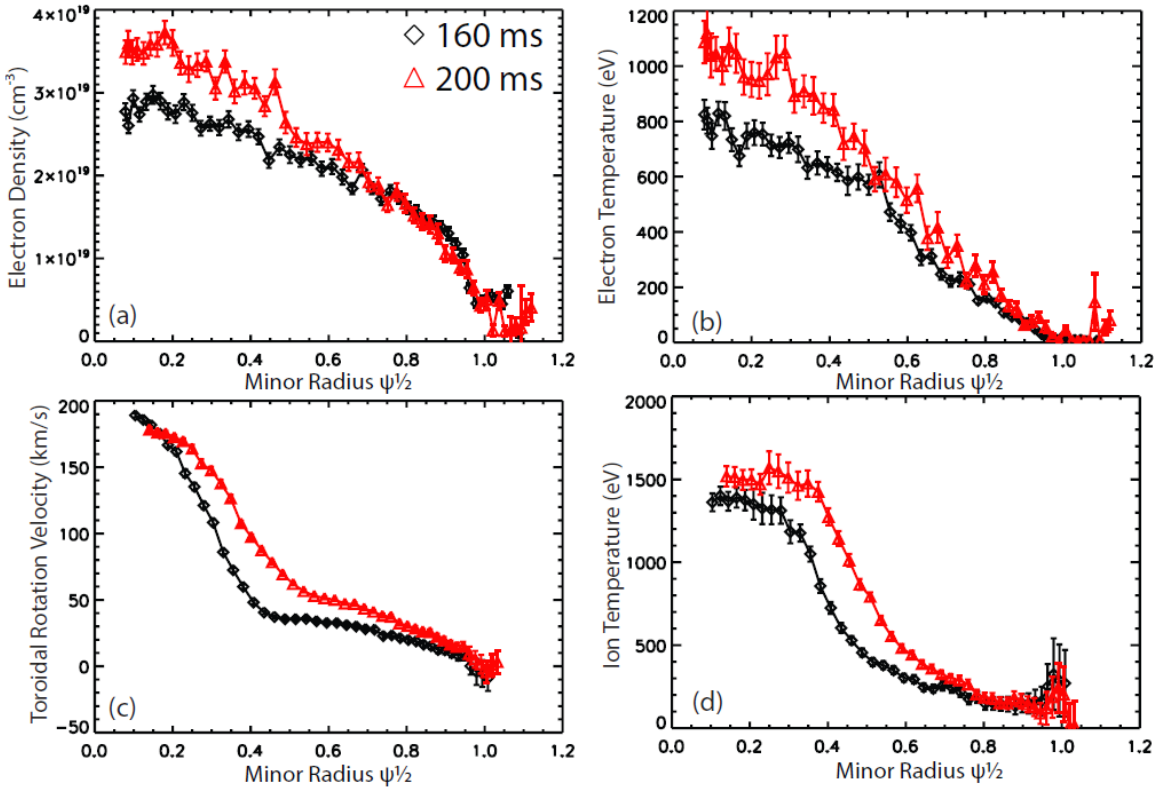

DBS vs. BES vs. CXRS velocities agree reasonably, except far in core

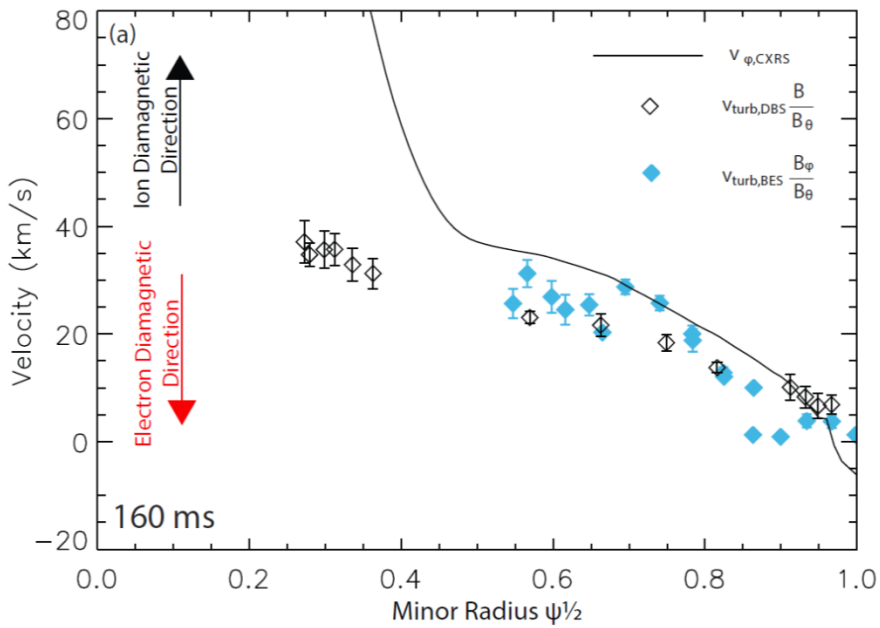

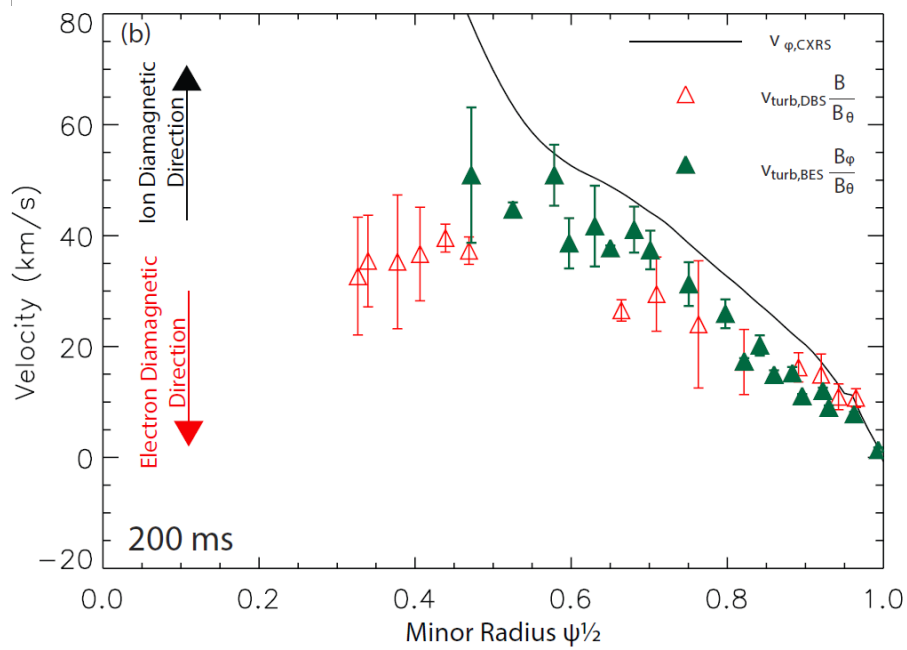

$$v_{turb,DBS} = v_{E\times B} + \cancel{v_{phase}}$$

$$E_r = \cancel{\frac{\nabla P_i}{e n_i}} + v_\phi B_\theta - \cancel{v_\theta B_\phi},$$

DBS vs. CXRS E_r comparison also shows reasonable agreement, except far in core

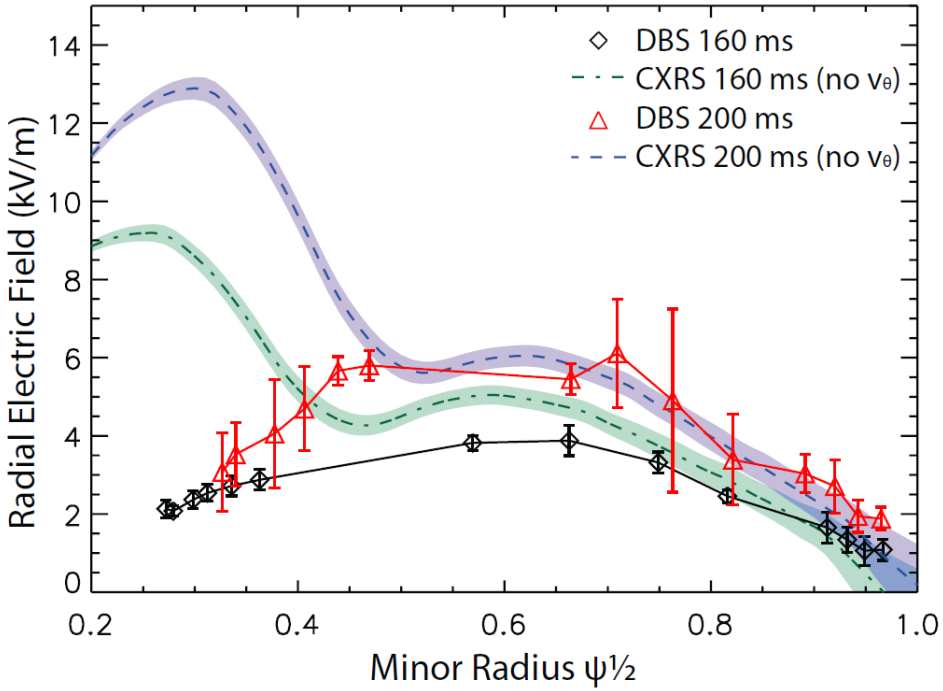

$$v_{turb,DBS} = v_{E\times B} + \cancel{v_{phase}}$$

$$E_r = \frac{\nabla P_i}{e n_i} + v_\phi B_\theta - \cancel{v_\theta B_\phi},$$

- Reasonable agreement, except inside of ITB
  - Poloidal rotation of ~15 km/s, significantly larger than neoclassical predictions, would be needed for agreement at $\sqrt{\psi}\approx 0.3$, observations of similar magnitude have been observed before in MAST (Field PPCF 2009)

Part I Summary

- DBS implementation for MAST was successful
  - 1st core DBS measurements in an ST & 1st independent 2D steering
  - Scattering calculations show good qualitative agreement with measurements
  - Data gathered on multiple topics

- **Demonstration of sensitivity to local magnetic field pitch angle with toroidal angle scans**
- **Demonstrated high-k measurements**
- **Velocity comparisons in reasonable agreement,** except inside an ITB where the inferred poloidal velocity is larger than neoclassical theory would predict

PART II:

Dependence of intrinsic rotation on collisionality in MAST

It is necessary to understand intrinsic rotation to predict performance of future devices

- Neutral beams used in existing experiments drive large toroidal flows, which stabilize instabilities like resistive wall modes and whose shear can suppress turbulent transport
- NBI is not expected to drive same levels of rotation in large future devices like ITER and DEMO, so understanding sources and underlying physics of intrinsic rotation is important
- Intrinsic rotation has been observed to reverse direction with ~10% changes in density in large aspect ratio experiments, which has been for many years unexplained

Rotation measurements with and without NBI

- Experimentally, intrinsic rotation in MAST can be on the same order as an NBI source, here ~1/2 the magnitude
- DBS is an ideal diagnostic for intrinsic rotation studies
  - Non-perturbative

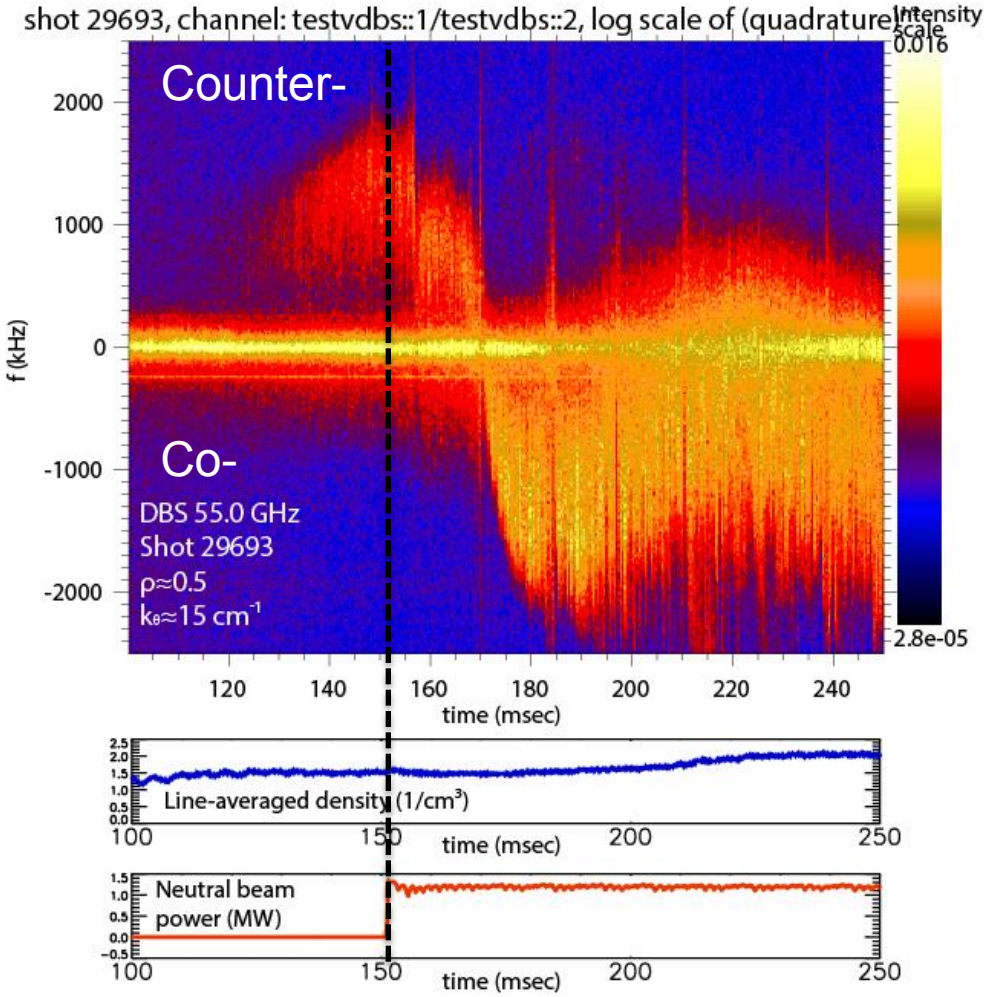

Ohmic intrinsic rotation reversals observed

- Core rotation in Ohmic plasma changes by order ~10 km/s with ~20% change in density

- **1st time observed in an ST**

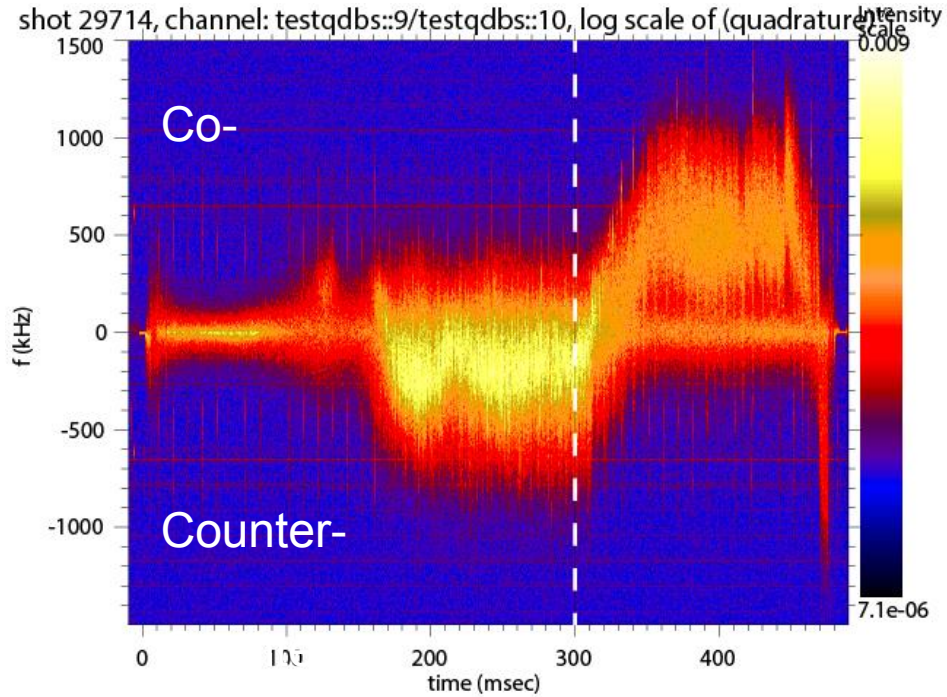

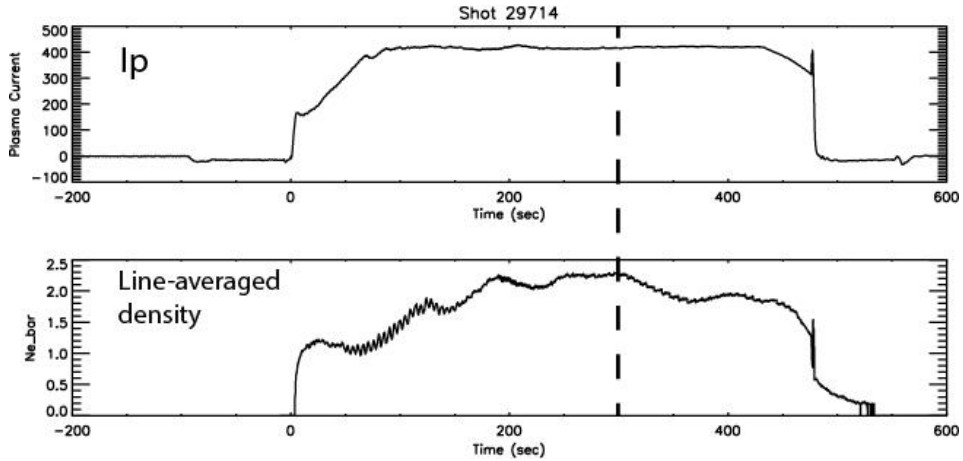

Ohmic rotation reversals background

- Observed in TCV (Bortolon PRL 2006), Alcator C-mod (Rice PRL 2011), and ASDEX-U (Angioni PRL 2011)
  - Line averaged-density at transition scales linearly with plasma current, suggesting collisionality dependence
- Explanation based on idea that reversal caused by transition in linear drive from ITG to TEM (Angioni PRL 2011)
  - Tests of this idea have shown little concrete support (White PoP 2013, Shi PoP 2013, Reinke PPCF 2013, McDermott NF 2014)
- Theory-based explanation based on impact of finite drift orbit effects on turbulent fluctuations (Barnes PRL 2013)
  - Not compared to experiment before now
  - Work here in collaboration with F. Parra & M. Barnes for comparison

Intrinsic rotation reversals predicted due to collisionality dependence

- Barnes et al., found mechanism for turbulent momentum flux that changes sign dependent on collisionality (Barnes PRL 2013)
  - Collisionality modifies neoclassical part of equilibrium ion distribution function
  - Interaction between finite orbit widths, density & temperature gradients, and collisions causes momentum transport

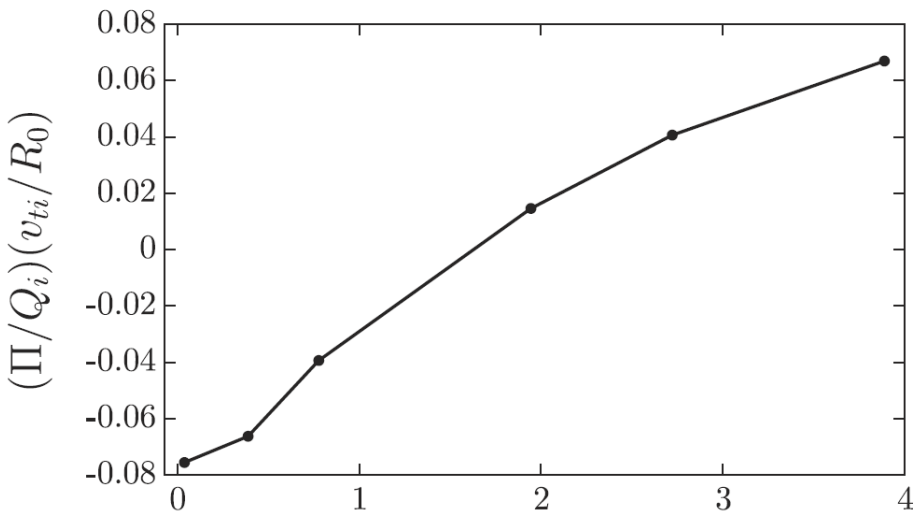

$$\nu_* = \frac{q\sqrt{\langle R^2\rangle}\nu_{ii}}{v_{ti}\epsilon^{3/2}}$$

- **Key physics:**
  - Magnitude of rotation should scale with size of diamagnetic effects
  - Can only change sign across transition from plateau regime to banana regime

Model for intrinsic momentum flux

$$\frac{v_{ti}}{\sqrt{\langle R^2\rangle}}\frac{\Pi_{int}}{Q_i} = \frac{v_{ti}}{\omega_{ci}}\frac{B}{B_\theta}\frac{1}{L_{T_i}}f(\nu_*)$$

$$\nu_* = \frac{q\sqrt{\langle R^2\rangle}\nu_{ii}}{v_{ti}\epsilon^{3/2}} \qquad \nu_{ii} = \frac{4\pi n_i e^4 \ln\Lambda}{\sqrt{m_i}(2T_i)^{3/2}}$$

$$f(\nu_*) = \frac{\widetilde{\Pi}_0\left(\frac{\nu_*}{\nu_c} - 1\right)}{1 + \frac{\nu_*}{\nu_c}\frac{\widetilde{\Pi}_0}{\widetilde{\Pi}_\infty}}$$

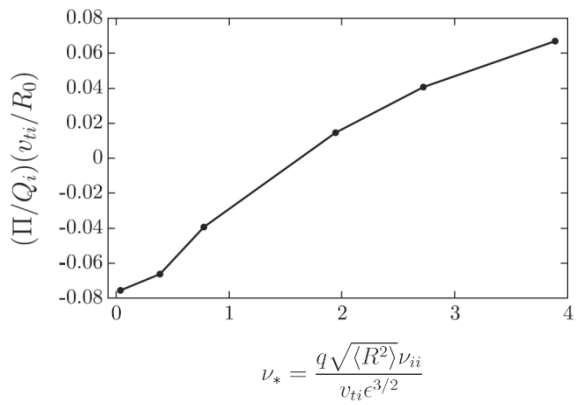

Parameter	CBC Value
$\widetilde{\Pi}_0$	0.3
$\widetilde{\Pi}_\infty$	1
ν_c	1.7
$\Omega_\phi(1)$	0

1D Analytical Model for intrinsic rotation profile

$$m_i n_i \chi_\phi \langle R^2 \rangle \frac{\partial \Omega_\phi}{\partial r} = \Pi_{int}$$

$$P_r = \frac{\chi_\phi}{\chi_i} \qquad n_i \chi_i \frac{\partial T_i}{\partial r} = Q_i$$

$$\frac{\partial \Omega_\phi}{\partial r} = \frac{v_{ti} \rho_{*,\theta}}{2 P_r L_{T_i}^2} f(\nu_*) \qquad \rho_{*,\theta} = \frac{v_{ti}}{\sqrt{\langle R^2 \rangle} \omega_{ci}} \frac{B}{B_\theta}$$

$$v_{tor}(\rho) = R \int_1^\rho \frac{\partial \Omega_\phi}{\partial \rho} d\rho + R\Omega_\phi(1)$$

- Intrinsic flux balanced by diffusion in steady-state
- Pinch and density gradient neglected for simplicity
- Turbulent Prandtl number taken to be 0.7
- For Ohmic plasmas assume T_e=T_i, n_e=n_i
- No parameters fit to data
- Due to approximations, restrict comparison to robust predictions; namely: the sign

Model reproduces qualitative changes in rotation

- DBS data show increase in core toroidal rotation towards co-current direction co-incident with change in density
- Time scale for rotation same as time scale for density
- Model predicts change in sign for core toroidal rotation, using EFIT and TS as inputs

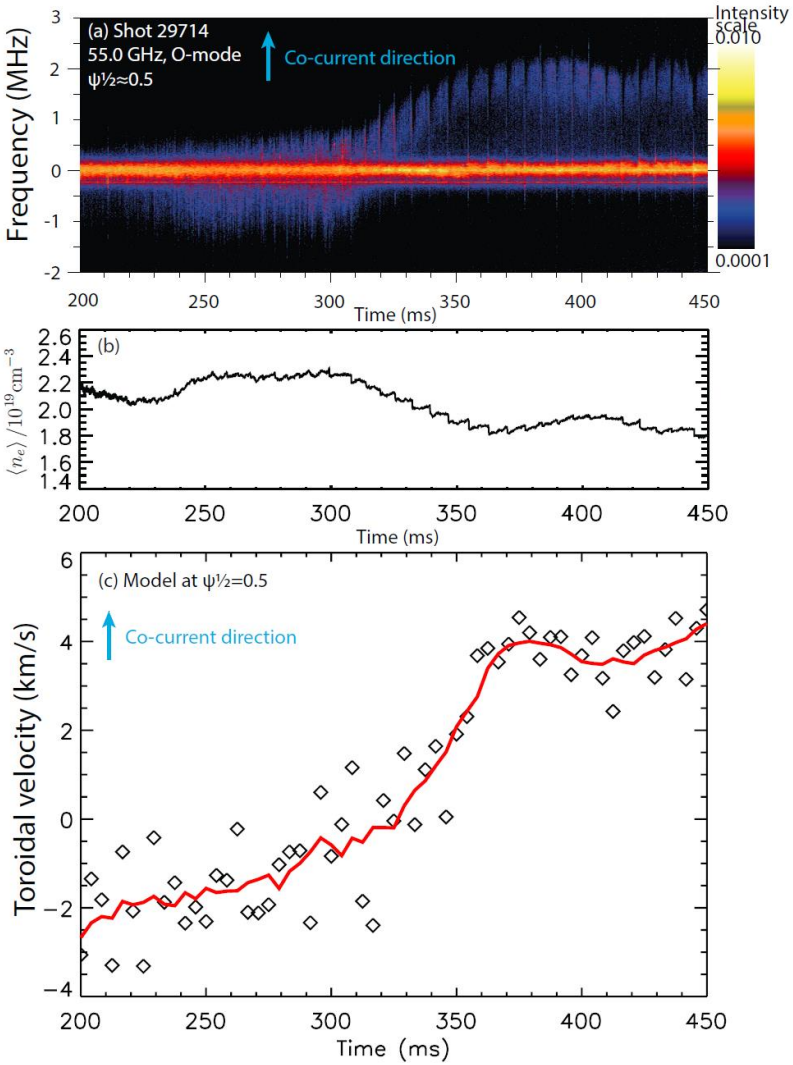

Model reproduces change towards co-rotation across profile

- Comparison across profile shows model predicts similarly shaped profiles as observed in experiment
- Difference found for magnitude
  - Model parameters from CBC
    - With factor ~x2-x3 change to Π_0, after accounting for difference at edge, model can match magnitude
  - Coriolis pinch might also explain difference
- Model does not account for changes in edge rotation

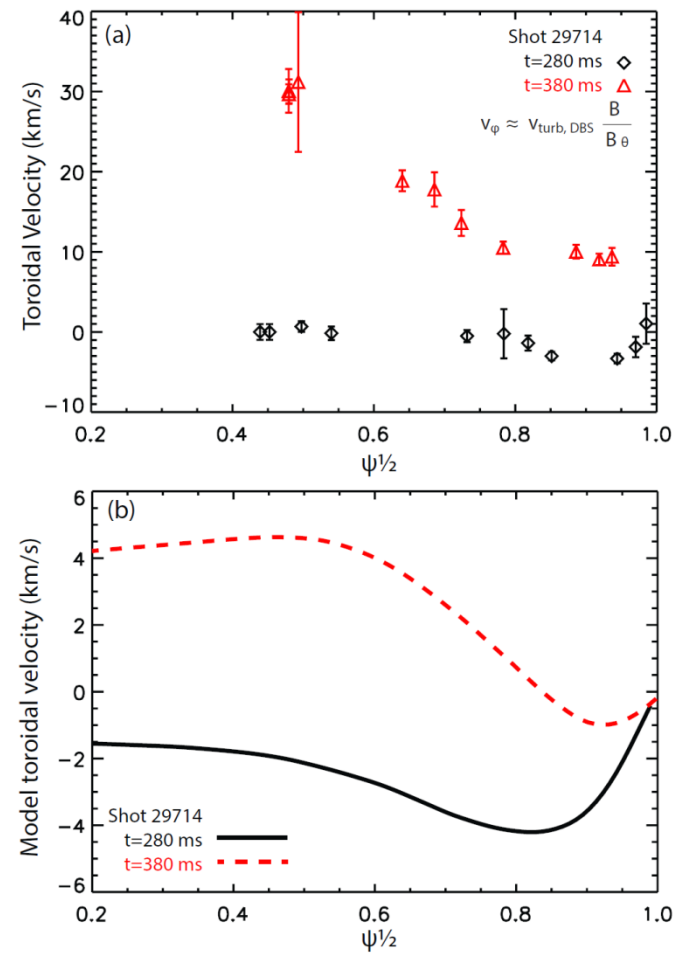

Collisionality profile determines rotation reversals

$$\frac{\partial \Omega_\phi}{\partial r} = \frac{v_{ti}\rho_{*,\theta}}{2P_r L_{T_i}^2} f(\nu_*) \qquad f(\nu_*) = \frac{\widetilde{\Pi}_0\left(\frac{\nu_*}{\nu_c} - 1\right)}{1 + \frac{\nu_*}{\nu_c}\frac{\widetilde{\Pi}_0}{\widetilde{\Pi}_\infty}}$$

- Controlling factor for reversals is movement of the radius where $\nu_* = \nu_c$

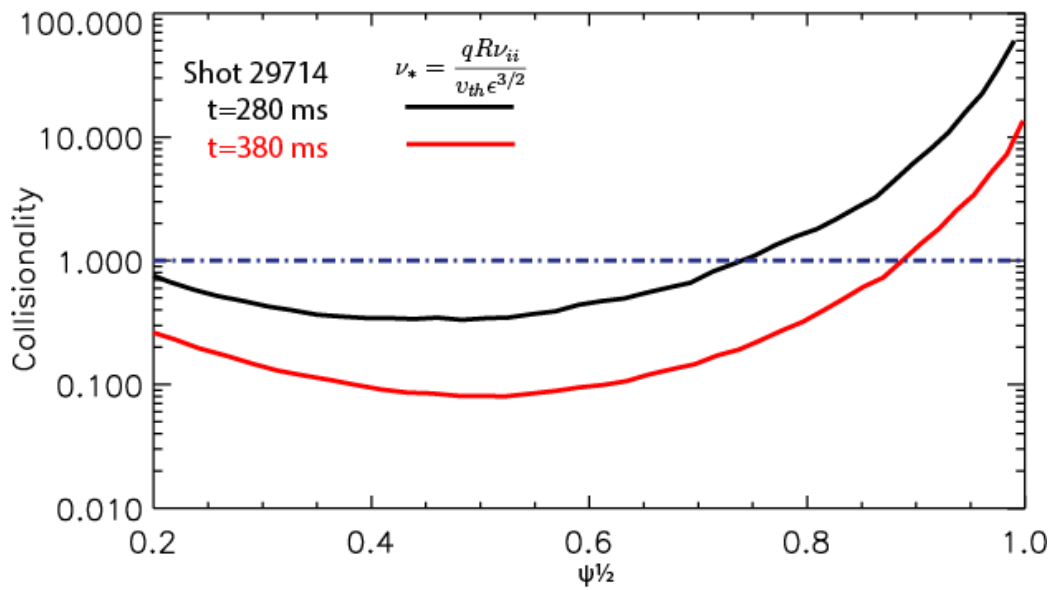

Model generally reproduces trend of increasing reversal density with current

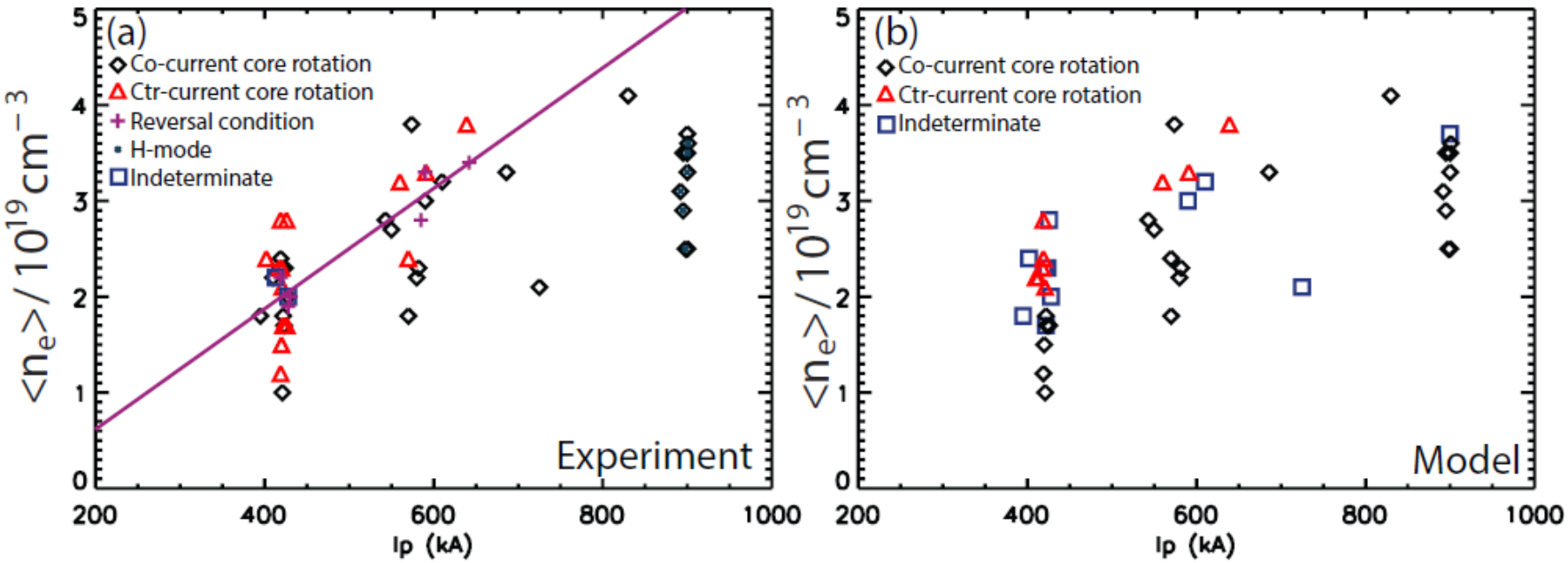

- Database includes Ohmic L-mode & H-mode, DND & LSND plasmas
- Reversal density increasing with current observed in C-mod, AUG, and now MAST
  - Model reproduces this trend

Model and experiment agree over most of database

- Model correctly reproduces sign of core toroidal rotation for ~80% of non-indeterminate cases
- Some cases near reversal conditions could be attributed to using CBC parameters
- Cases at low current and low density appear to be robustly outside of explanation by model

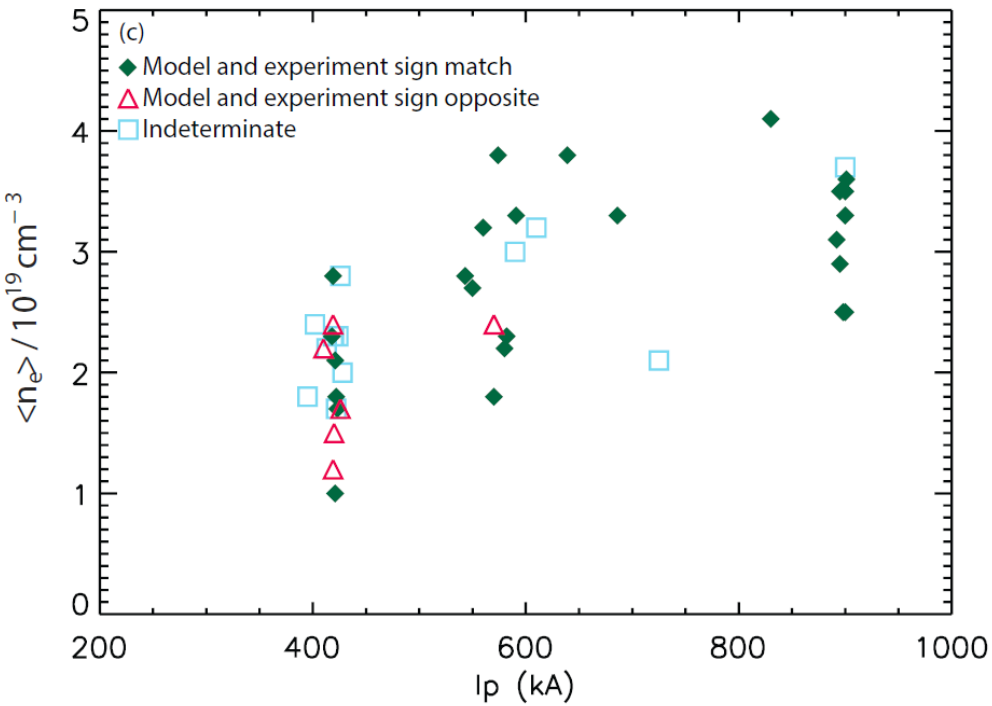

Part II Summary

- Intrinsic rotation reversals observed for the first time in a spherical tokamak
  - Unlike conventional tokamaks, we also observe a change in edge rotation

- 1D analytical model for intrinsic rotation developed, which captures collisionality dependent finite drift orbit effects on turbulence

- Good agreement for sign of toroidal rotation over database of Ohmic plasmas

PART III:

Cross-Polarization DBS and Microtearing at the Top of the MAST H-mode Pedestal

Microtearing predicted to be linearly unstable in the MAST pedestal

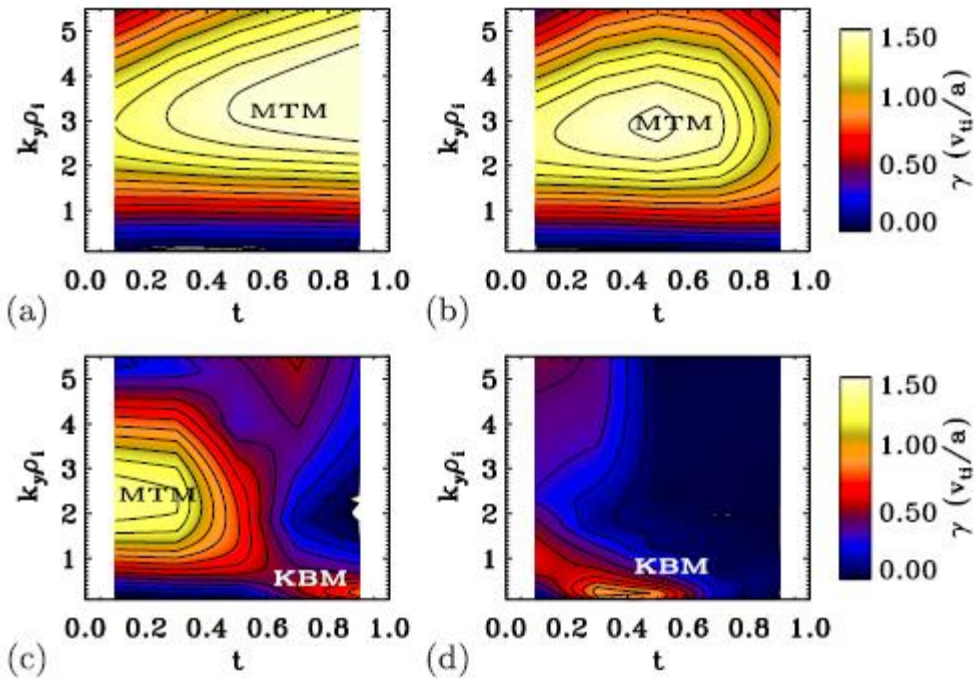

FIG. 3 (color online). $\gamma(k_y\rho_i, t)$ over the ELM cycle at $\Psi_N = 0.95, 0.96, 0.97, 0.98$ in (a)–(d), respectively. γ is normalized to v_{ti}/a, v_{ti} is the local ion thermal velocity, and a is the minor radius.

Dickinson PRL 2012

- Microtearing modes predicted to be unstable in MAST
  - At wavenumbers DBS can measure
  - At radii DBS can measure

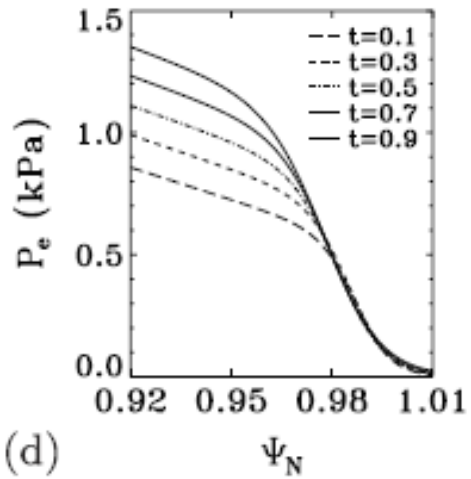

Cross-polarization scattering is sensitive to magnetic field fluctuations and has been used in previous work

$$-\nabla \times (\nabla \times \mathbf{E}_s) + \left(\frac{\omega_i}{c}\right)^2 \left(1 - \frac{\sigma}{i\varepsilon_0\omega_i}\right)\mathbf{E}_s = -i\mu_0 \frac{\partial \mathbf{J}^{(2)}}{\partial \mathbf{t}}$$

$$\mathbf{J}^{(2)} = \frac{i\varepsilon_0\omega_{pe}^2}{\omega_i}\frac{\tilde{n}}{n_e}\mathbf{E}_i + \frac{\omega_i}{\varepsilon_0\omega_{pe}^2}\sigma[(\sigma\mathbf{E}_i) \times (\tilde{B}/B)]$$

Standard scattering

Cross-polarization scattering

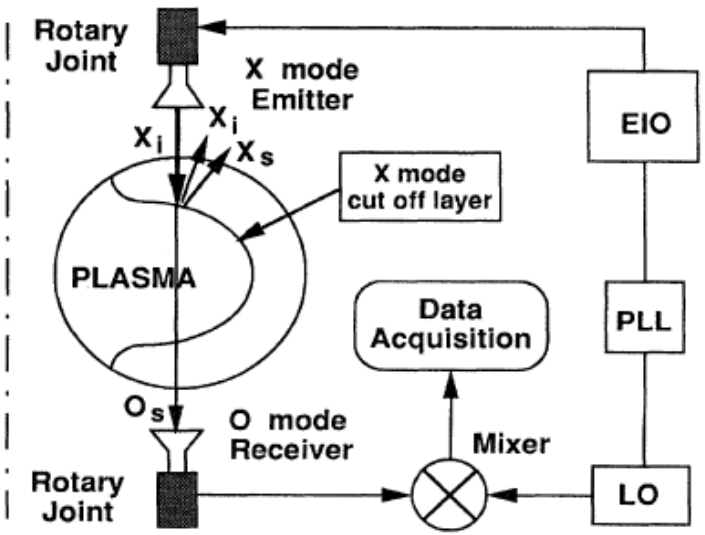

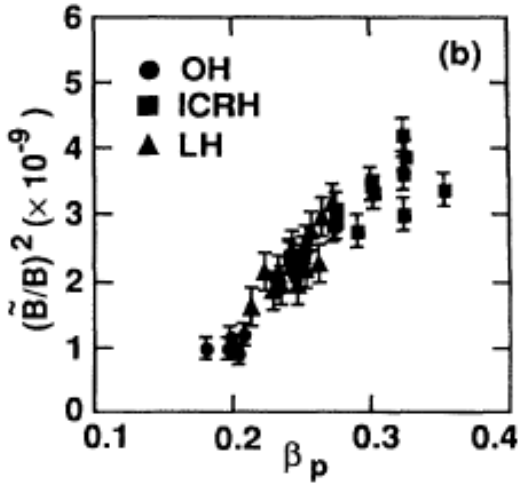

- Above and right from Zou PRL 1995
  - Also see Lehner EPL 1989, Vahala PFB 1992, Bruskin PPCF 1994, and others
- Same concept recently implemented at DIII-D by T.L. Rhodes et al.

DBS system reconfigured during last week of campaign

Standard configuration DBS (same antenna for launch and receive)

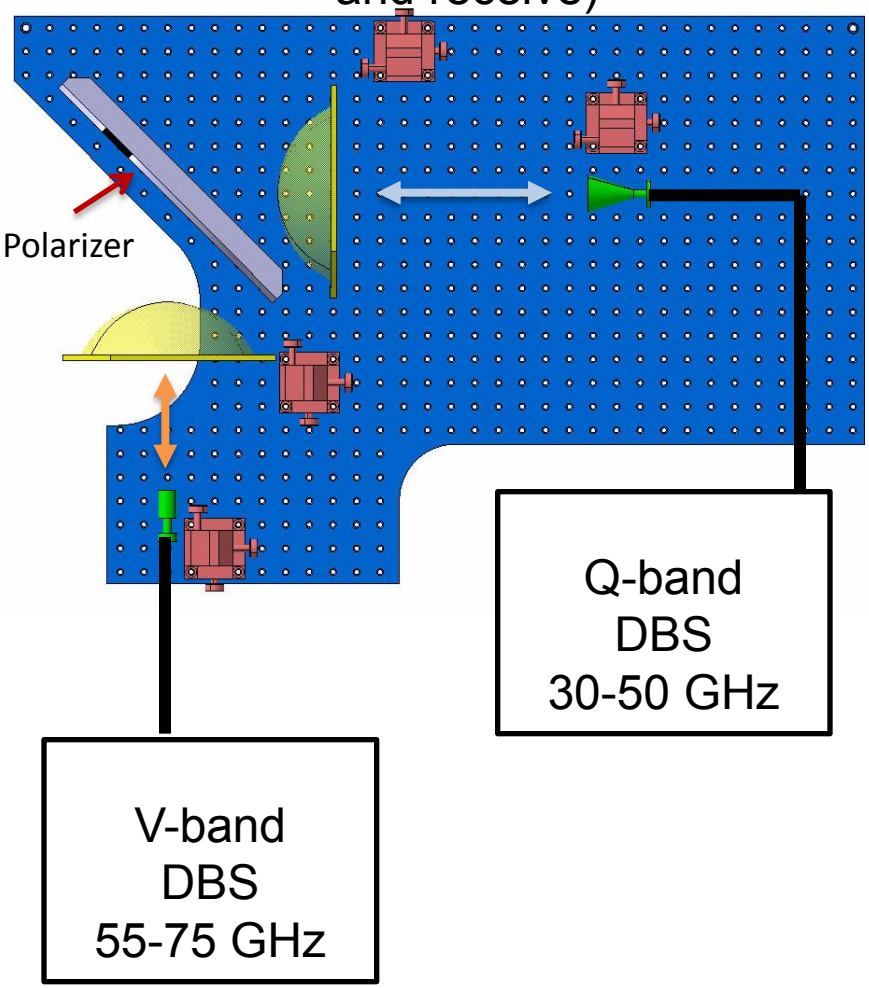

Cross-polarization DBS (launch and receive orthogonal polarizations)

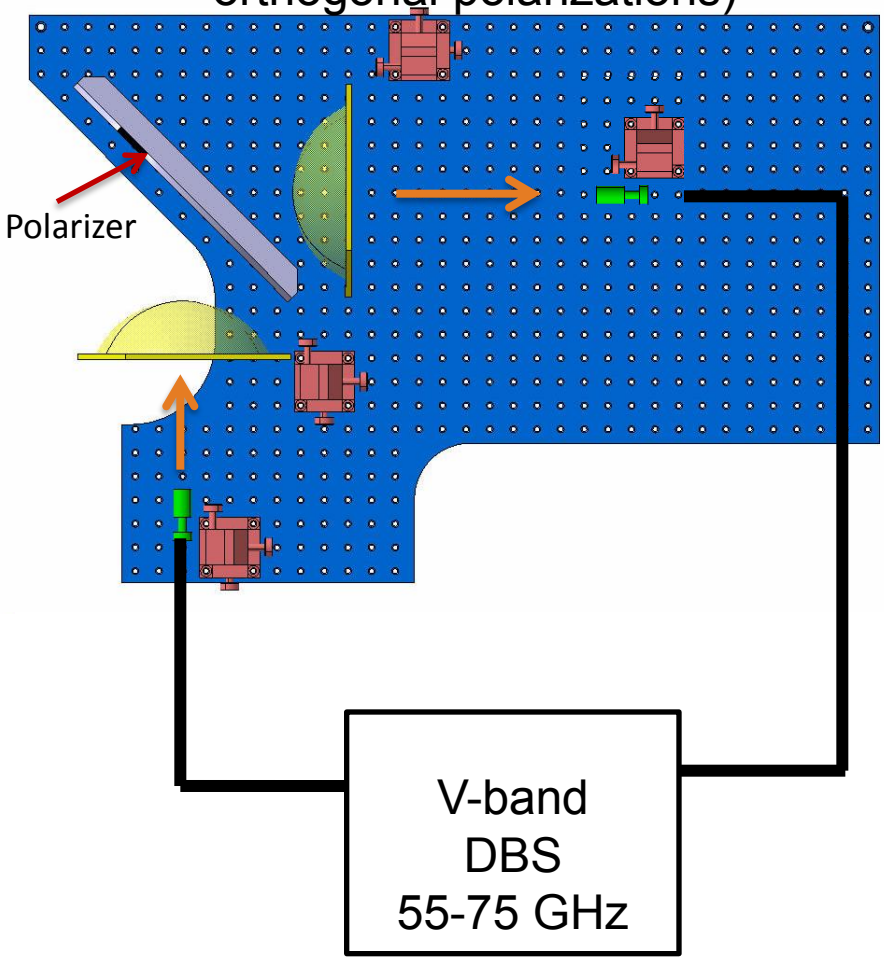

Scattering efficiencies, polarization alignment, and ratio of fluctuation levels impact interpretation of CP-DBS

- CP-DBS attempted with X-mode launch, O-mode receive
  - Plasma modeled in Dickinson PRL 2012 repeated

- Diagnostic setup acts as system of beam splitters
  - Two passes through polarizer plus plasma itself, due to any polarization misalignment
  - $(\delta B/B)/(\delta n/n)$ expected to be at most ~10^{-1} to 10^{-2}
  - X→O scattering efficiency must be compared to O→O, with estimate of residual launched O-mode from polarization mismatch, other possible X→O conversion mechanisms (e.g. propagation in steep gradients), and estimate of received X→X due to polarization mismatch
  - Simple argument in next few slides that polarization mismatch can be inferred from the data itself in an ST

Isolating magnetic fluctuations

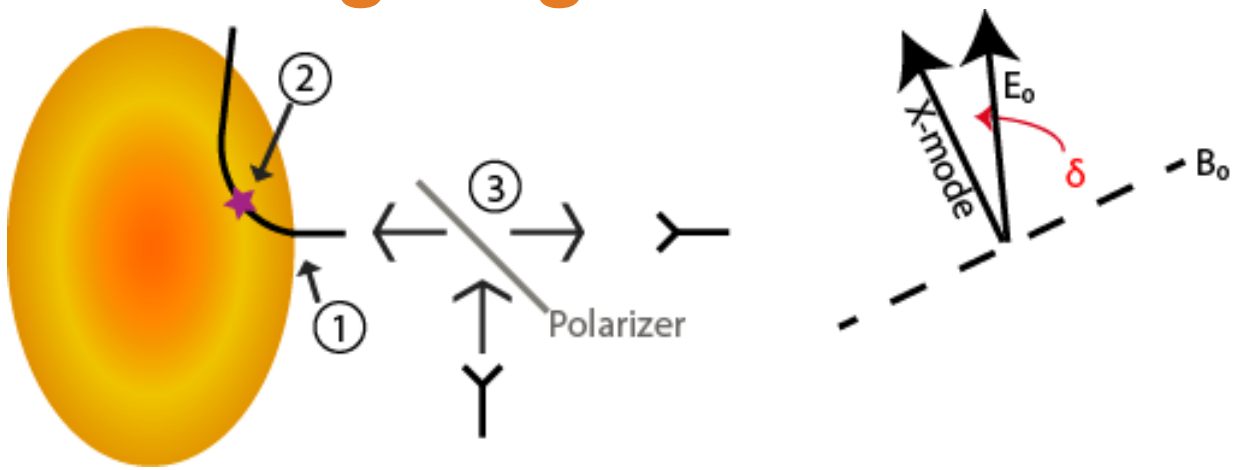

1.Polarization mismatch

$$X \rightarrow \cos^2\delta$$

$$O \rightarrow \sin^2\delta.$$

2.Scattering efficiencies

$$S_{X\rightarrow O}\cos^2\delta$$

$$S_{X\rightarrow X}\cos^2\delta$$

$$S_{O\rightarrow O}\sin^2\delta$$

3. Polarizer rejection

$$P_{B,O} = S_{X\rightarrow O}\cos^2\delta\cos^2\delta$$

$$P_{n,X} = S_{X\rightarrow X}\cos^2\delta\sin^2\delta$$

$$P_{n,O} = S_{O\rightarrow O}\sin^2\delta\cos^2\delta$$

- Contributions from each cutoff can be separated due to difference in Doppler shift

Two important ratios can be defined

$$P_{B,O} = S_{X\to O}\cos^2\delta\cos^2\delta$$

$$P_{n,X} = S_{X\to X}\cos^2\delta\sin^2\delta$$

$$P_{n,O} = S_{O\to O}\sin^2\delta\cos^2\delta$$

$$R_1 = \frac{P_{B,O}+P_{n,X}}{P_{n,O}} = \frac{S_{X\to O}\cos^2\delta + S_{X\to X}\sin^2\delta}{S_{O\to O}\sin^2\delta}$$

$$R_2 = \frac{P_{B,O}}{P_{n,X}} = \frac{S_{X\to O}}{S_{X\to X}}\frac{1}{\tan^2\delta}$$

$$R_2 = \frac{S_{O\to O}}{S_{X\to X}}R_1 - 1 \Rightarrow R_2 \approx R_1 \text{ if } \mathrm{R}_1 >> 1$$

- In an ST, due to low B, small difference between X-mode and O-mode cutoff
  - If polarization is poorly matched, should see both, with different Doppler shifts
- Ratio between power from each cutoff is related to ratio of power from X-mode cutoff due to density and magnetic field fluctuations

Degree of polarization mismatch can be determined from data

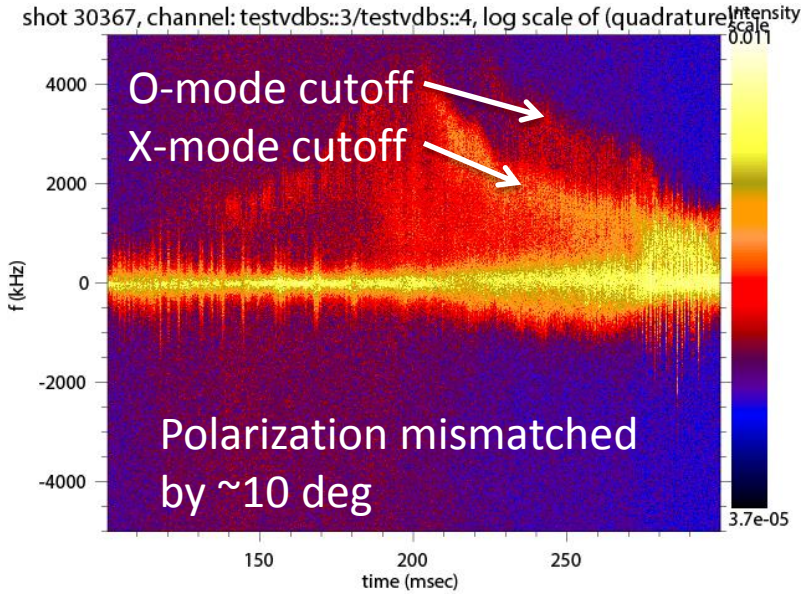

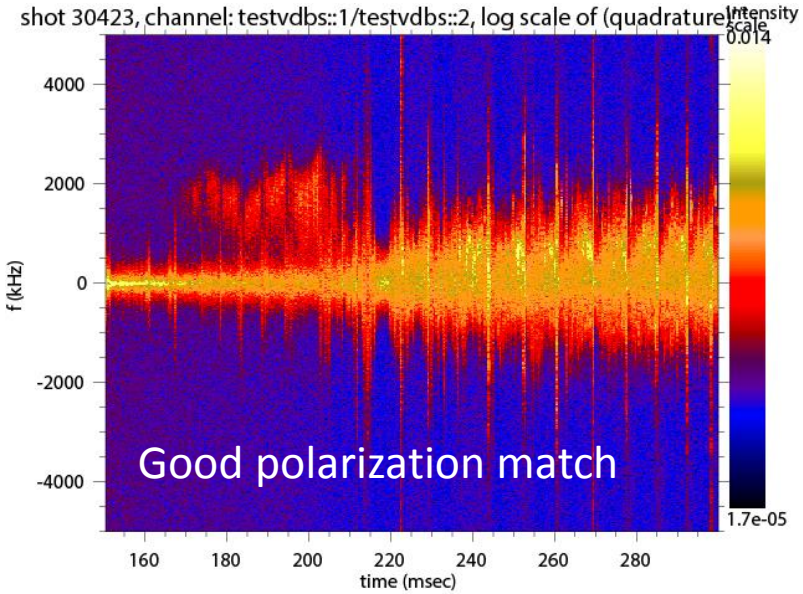

$$R_1 = \frac{P_{B,O} + P_{n,X}}{P_{n,O}}$$

Ratio in total power received from X- and O-mode cutoffs

$$R_2 = \frac{P_{B,O}}{P_{n,X}}$$

Ratio in power received due to $\tilde{B}$ and $\tilde{n}$ from X-mode cutoff

$$R_2 = \frac{S_{O\to O}}{S_{X\to X}} R_1 - 1 \Rightarrow R_2 \approx R_1 \text{ if } \mathrm{R}_1 >> 1$$

- Lack of 2nd peak implies good polarization match, i.e. the measurement is sensitive to magnetic field fluctuations

Strong CP-DBS signal in plasma where MTM predicted unstable

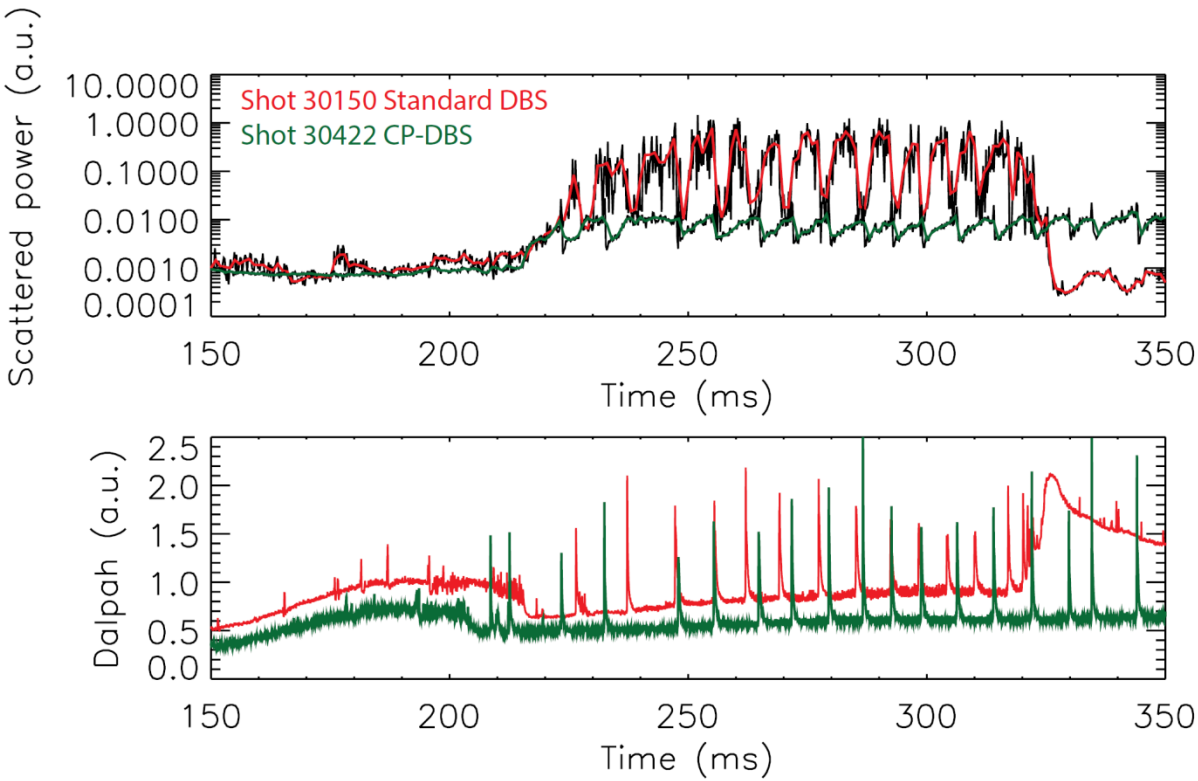

- Target plasma:
  - Type I ELMs
  - β_n~4.0-4.5
- Standard DBS signal much larger than CP-DBS signal
- Different temporal evolution

- Strong signal dominated by magnetic fluctuations measured at wavenumber and location where MTM predicted unstable
- Little signal in any other plasma conditions

Part III Summary

- Argument presented that it is possible to tell from the data itself in an ST how well polarization is matched for CP-DBS

- Strong signal dominated by magnetic field fluctuations measured at top of MAST H-mode pedestal at wavenumbers and position where MTM had been predicted unstable

- Further work ongoing

Overall Summary

- First successful implementation of DBS for core measurements in a spherical tokamak
  - Demonstrated high-k measurements and sensitivity of local magnetic field pitch angle with 2D steering
  - arXiv:1407.2115

- Good agreement for model describing collisionality dependence of Ohmic intrinsic rotation reversals
  - arXiv:1407.2121

- Data consistent with MTM at top of pedestal between Type I ELMs obtained